Conf-900513--3

Solid–Particle Erosion of Aluminum/Particulate Ceramic Composites*

K. C. Goretta, W. Wu, and J. L. Routbort
Argonne National Laboratory, Argonne, IL 60439
and
P. K. Rohatgi
University of Wisconsin–Milwaukee, Milwaukee, WI 53201

CONF-900513--3

DE91 006078

June 1990

Paper presented at the Tribology of Composite Materials, May 1–3, 1990, Oak Ridge, TN.

*This work was supported by the U. S. Department of Energy, Office of Basic Energy Sciences, Division of Materials Science, under Contract W–31–109–Eng–38. The Al alloy and Al/SiC composites were provided by D. J. Lloyd of Alcan International and the Al/Al_2O_3 composites were provided by T. Klimowicz of Dural Aluminum.

Solid–Particle Erosion of Aluminum/Particulate Ceramic Composites

K. C. Goretta, W. Wu, and J. L. Routbort
Argonne National Laboratory, Argonne, IL 60439
and
P. K. Rohatgi
University of Wisconsin–Milwaukee, Milwaukee, WI 53201

ABSTRACT

Impact erosion of 2014 aluminum, 2014 aluminum + 20 vol.% particulate silicon carbide, and 2014 aluminum + 20 vol.% particulate aluminum oxide has been studied at room temperature. The alloys were tested in the as–received and heat–treated conditions. Experiments were conducted with aluminum oxide abrasive in vacuum in a slinger–type apparatus over a range of abrasive size, velocity, and angle of impact. Erosion rates were influenced by reinforcement and heat treatment. Reduced ductility, both overall and local, attributed to reinforcement or heat treatment, caused, under most conditions, more rapid erosion of the composites. The data suggest that erosion rate can be minimized by proper microstructural control, involving reducing reinforcement segregation and the amount of intermetallic compounds.

EROSION by solids entrained in gas streams can cause severe damage in systems such as gas turbines, cyclone generators, fluidized beds, and boilers [1]. Erosion of structural materials has been studied extensively and much is known about erosion of metals and monolithic ceramics [2,3]. Metal– and ceramic–matrix composites with superior mechanical properties have been developed recently [4–7]. The erosion behaviors of these advanced materials are now being investigated. This paper will present results of experiments on erosion, by a stream of aluminum oxide abrasive, of cast 2014 aluminum, 2014 aluminum + 20 vol.% particulate silicon carbide, and 2014 aluminum + 20 vol.% particulate aluminum oxide.

BACKGROUND

Solid–particle erosion of metals occurs by a combination of cutting, gouging, tearing, and ploughing [2,3]. The rate at which material is removed from a target is dependent on the properties of both erodent and target and on the impact conditions: angle of impact and velocity and size of impacting particles [2,3,8]. Because the erosive processes are more efficient for oblique angles of incidence, maximum material removal in metals generally occurs at about 20° and minimum removal occurs at 90° [3,8]. Hard metals with limited ductility constitute an exception to this rule. For metals such as hardened steel [9] or electroless nickel [10], maximum erosion rates occur at angles approaching 90°.

Material removal in ceramics is dependent on the shape of erodent. Blunt particles create Hertzian cracks, which are cone shaped [3,11], and sharp particles create radial and lateral cracks [3,12–15]. Herzian cracks nucleate at existing flaws in the ceramic. The process is elastic and can be described by linear elastic fracture mechanics [3,11]. Cracking induced by sharp particles involves both elastic and plastic deformation. The process is analogous to an indentation test. Impact creates a zone of plastic deformation beneath the impacting particle. The resultant stress causes formation of a radial crack. As the impacting particle recoils, unloading produces tensile stresses below the plastic zone. These stresses cause lateral cracks to propagate parallel to the surface. Material removal results when the lateral cracks extend to the surface [3,12,13].

Maximum erosion rates for ceramics occur at 90° [3,12–15]. Models of the erosion process, which take into account only the normal component of the erodent velocity, are successful in predicting erosion rates for normal incidence. Erosion rates for oblique incidence should be proportional to the normal component of velocity, $V\sin\alpha$, where V is the velocity and α the angle of impact [3]. It has been found, however, that oblique erosion rates are higher than predicted by the models. The higher rates appear to be the result of two contributions to material removal that are not considered in the models: plasticity [3,16] and cracking from Mode II or III loading [3,17].

Erosion is not understood as well for composite materials as it is for metals and ceramics [14,15,18]. Several questions require experimental investigation. Among them are the extent to which erosion of fiber reinforced and particle reinforced composites is similar; the effects of reinforcement composition and distribution on erosion; the effects of matrix properties on erosion; whether consistent relationships exist between erosion rate and angle of impact; and whether erosion of metal–matrix composites can be adequately represented by a power law expression of erodent size and velocity. To address these questions, solid–particle erosion of 2014 Al has been studied. The alloy was reinforced with 20 vol.% particulate SiC or Al_2O_3. The materials were tested in the as–cast and T6 heat–treated conditions. The goals of this work were to identify which microstructural features have the greatest influences on erosion and to provide recommendations for alloy design.

EXPERIMENTAL DETAILS

The three materials tested [18,19] each had a primary grain size of 15–25 µm. The SiC particles were approximately ellipsoidal. Small regions of tightly agglomerated particles were present, however, and in many of these regions, the Al matrix did not completely fill the space between particles. The Al_2O_3 particles were about the same size as the SiC. The particles were slightly more segregated on a gross scale, but fewer tight agglomerates were present and almost no large voids were observed. These microstructures are typical of cast aluminum–matrix composites. Aluminum dendrites form and the reinforcement particles are forced into interdendritic regions (Fig. 1).

The base alloy (Al) and the SiC composite (Al/SiC) were tested in the as–cast and T6 heat–treated conditions. The Al_2O_3 composite (Al/Al_2O_3) was tested in the T6 condition only. The T6 heat–treated specimens were heated in air to 502°C, held at temperature for 1 h, water quenched to 25°C, tempered in air for 16 h at 160°C. For each material, density was determined by the Archimedes method, Vicker's hardness, Hv, was measured with a 10–kg load, and Young's modulus was measured ultrasonically [20].

Erosion specimens were cut from billets by diamond saw and then ground flat with 400–grit SiC paper. The surfaces used for erosion testing were approximately 19 mm x 27 mm. Erosion tests were conducted at room temperature, in vacuum, in an apparatus that has been described [21]. The erodent used was commercial angular Al_2O_3 (Norton Alundum 38), average particle size, D, of 23, 42, 63, 143, or 390 µm. Erodent velocities, V, were 50, 75, or 100 m/s and angles of impact, α, ranged from 10 to 90°. The specimens were weighed to the nearest 0.1 mg, subjected to erosion, cleaned ultrasonically in methanol, and then reweighed. Steady–state erosion was determined as the mass lost from the target per mass of impacting particles. At least five erosion cycles were performed to define the steady state. Scanning electron microscopy (SEM) was performed on each steady–state surface. In addition, several specimens were polished to a 1–µm finish and eroded with only a few particles so that individual impact sites could be examined by SEM.

RESULTS

The properties of the base alloys were affected by reinforcement and heat treatment. Young's modulus was 75 ± 2 GPa for the Al, 101 ± 1 GPa for the Al/SiC, and 95 ± 1 GPa for the Al/Al_2O_3. Hardnesses increased with reinforcement and heat

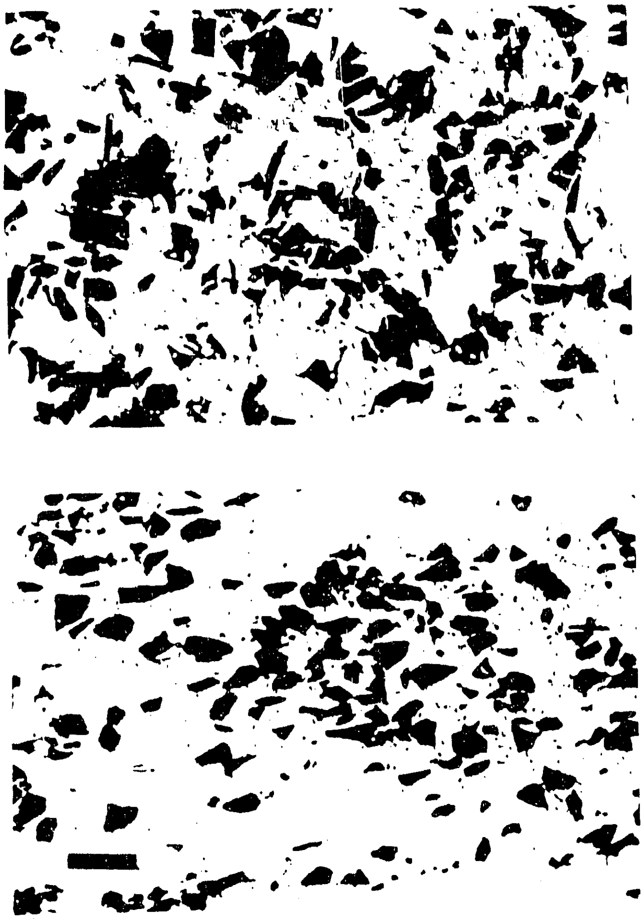

Fig. 1 – Optical micrographs of (a) as–cast Al/SiC and (b) as–cast Al/Al_2O_3; bars equal 50 μm.

treatment, as expected: as–cast Al = 98 Hv, T6 Al = 166 Hv; as–cast Al/SiC = 139 Hv, T6 Al/SiC = 188 Hv; and T6 Al/Al_2O_3 = 185 Hv.

A clear steady–state erosion rate, ΔW (expressed in mg of target removed per g of impacting particles), was established for each material. All of the composite specimens obtained steady state without appreciable transient response. The Al specimens exhibited little or no transients at low angles of incidence. For normal incidence, however, the specimens gained mass initially because of embedding of the erodent. Steady state was achieved only after long transients. Embedding was less severe for the heat–treated specimens and the transient periods were shorter.

The effect of angle of impact on ΔW was similar for all combinations of impact velocity, V, and erodent particle size, D. Representative data are shown in Fig. 2. For the Al, maximum erosion was always at 15° impact and minimum erosion at 90°. For the composites, the maximum erosion rate occurred from 15° to 30°, with the maximum for impact by smaller particles tending to occur at 15°; the minimum was always at 90°. The composites always eroded more rapidly than did the Al.

It was found that ΔW was proportional to V^n, where n is a semi–empirical exponent [3]. The data for n values for the various targets and angles of impact of 15, 30, and 90° are given in Table 1. The exponents ranged from 1.8 to 2.7, with most falling between 2.0 and 2.5. The exponents were generally higher for the heat–treated specimens and slightly lower for the composites. Little or no effect of angle was observed. Representative curves documenting fits to the data are shown in Fig. 3.

The effect of D on erosion rate was complex and a simple power–law expression could not be used. Figure 4 contains representative data gathered for a velocity of 75 m/s. All heat–treated specimens exhibited a saturation phenomenon in which the erosion rate was approximately independent of particle size for $D \geq 143$ μm. The as–cast specimens exhibited a bending of the ΔW vs D curves for large D, but not a saturation. Little difference was found between erosion of Al/SiC and Al/Al_2O_3. Heat treatment increased erosion rates substantially for normal impact, but had little influence for glancing impact.

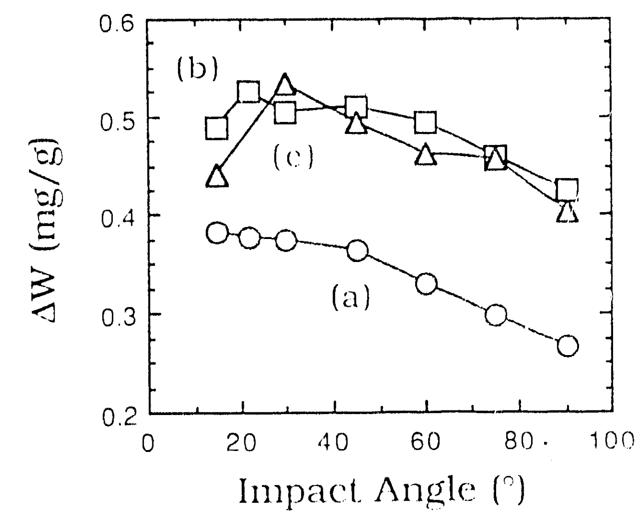

Fig. 2 – Steady–state erosion rates of heat–treated (a) Al, (b) Al/SiC, and (c) Al/Al_2O_3 for V = 75 m/s and D = 143 μm.

Table 1 – Velocity exponents for impact by 143 μm particles at different impact angles; the values are accurate to ± 0.2

Targets	Impact Angle (°)	n
2014 (as–cast)	15	2.0
	30	1.9
	60	1.9
	90	2.0
2014 Al (heat–treated)	15	2.5
	30	2.5
	90	2.5
Al/SiC (as–cast)	15	1.8
	30	2.0
	60	1.9
	90	1.9
Al/SiC (heat–treated)	15	2.2
	30	2.1
	60	2.3
	90	2.3
Al/Al_2O_3 (heat–treated)	15	2.7
	30	2.1
	90	2.2

The surfaces of the Al impacted at 15° had a smeared, gouged appearance. The Al/SiC and Al/Al_2O_3 surfaces were similar, but also contained many regions of ductile tearing (Fig. 5). The 90° surfaces lacked the oriented gouging of the 15° surfaces, but exhibited the same sort of general smearing. Significant tearing and many shear bands were apparent on the composite surfaces.

At oblique single impact sites in the Al, material was displaced forward, resulting in a piling up of metal at the front of a gouge. Very small tears were evident. In the Al/SiC and Al/Al_2O_3, tearing was much more prevalent and some of the reinforcement was fractured. The piling up of metal was reduced by the reinforcement particles (Fig. 6).

For impact at 90°, many of the damage sites in the Al were characterized by laterally displaced material. Some, such as Fig. 7a, exhibited material removal. In this figure, the intermetallic

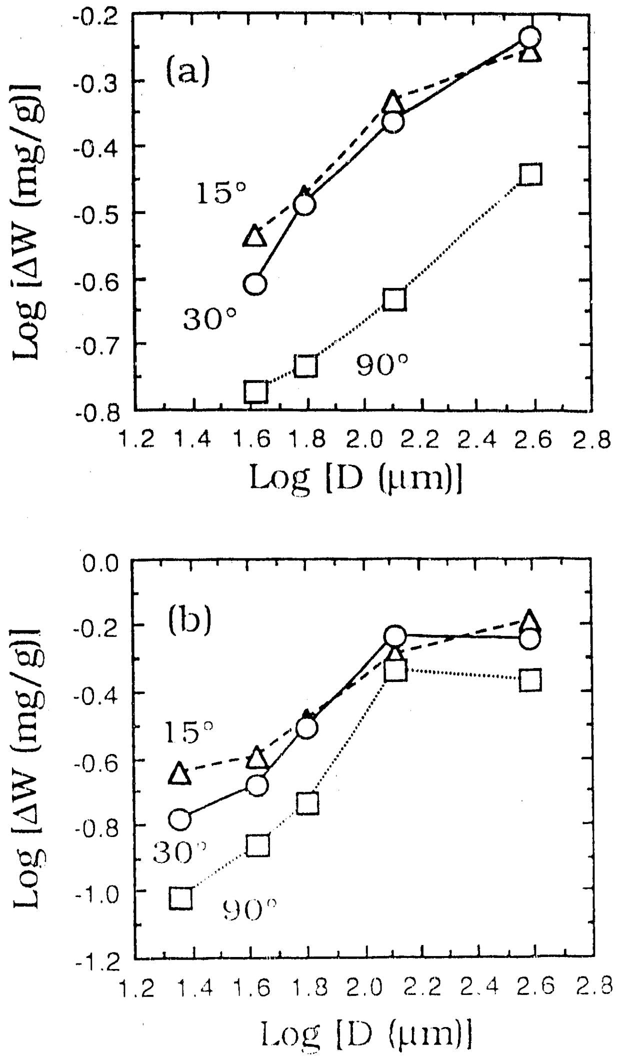

Fig. 3 – Steady–state erosion rates as a function of V with D = 143 μm for (a) as–received Al/SiC and (b) heat–treated Al/SiC.

inclusions in the Al were evident and were observed to act as initiation sites for small tears. The composites generally exhibited fractured reinforcement particles and removal of material with each impact. Regions of metal near clusters of reinforcement were most susceptible to removal. Figure 5b shows a region of material removal in which SiC particles formed a tight agglomerate below the surface. The material above this region was removed by a single impact. For small particles impacting at low velocities, material removal was only evident when these regions of constrained metal were struck.

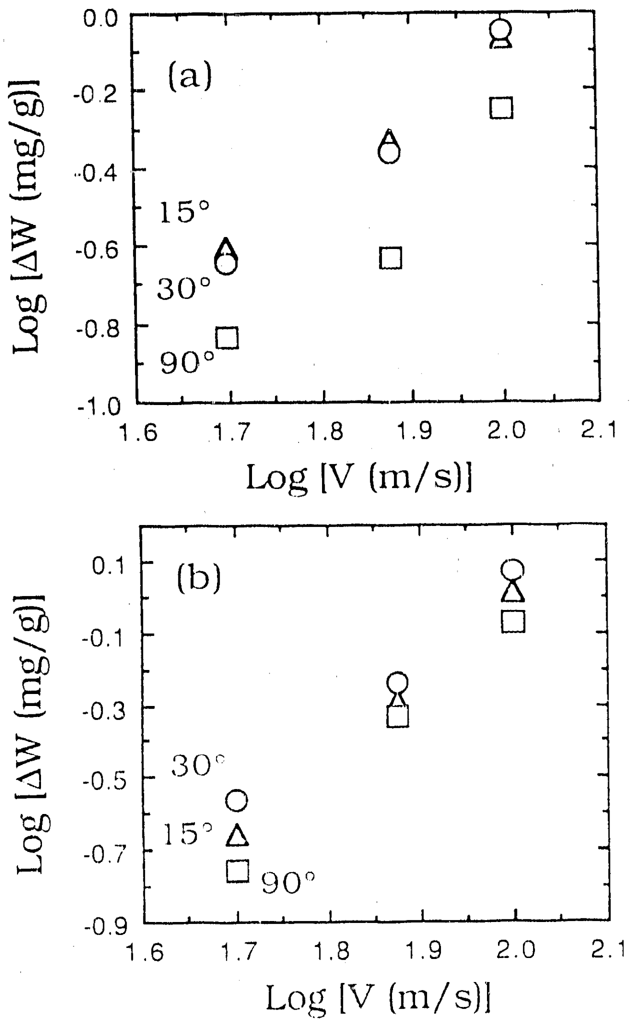

Fig. 4 – Steady–state erosion rates as a function of D for V = 75 m/s for (a) as–cast Al/SiC and (b) heat–treated Al/SiC.

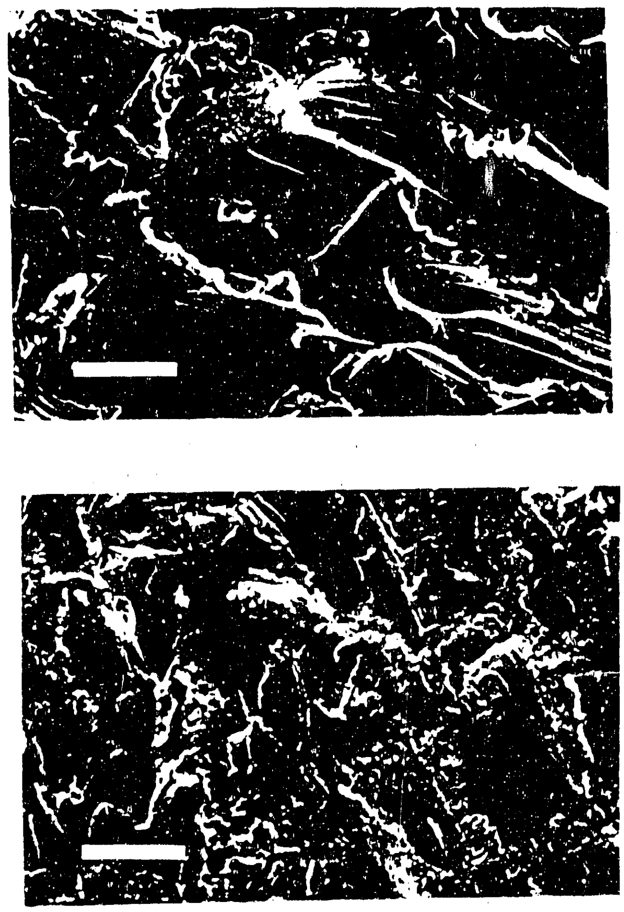

Fig. 5 – SEM micrographs of steady–state erosion surfaces for V = 75 m/s and D = 390 μm, (a) as–cast Al impacted at 30° and (b) as–cast Al/SiC impacted at 30°; bars equal 10 μm.

DISCUSSION

The composite materials consisted of a ductile metal reinforced with a brittle ceramic. The erosion rate of 2014 Al is about an order of magnitude higher than that of either SiC [23] or Al_2O_3 [14]. If some type of rule of mixtures described erosion of the composites, the expectation would be for lower erosion rates in the composites. However, for all combinations of α, V, and D, the composites had higher erosion rates than did the Al. This difference in rate, although never more than about 50%, is significant for any application in which erosion is likely to determine the life of a part.

Each of the materials exhibited maximum erosion at oblique incidence, and minimum erosion at normal incidence. As such, erosion of each appears to be primarily by a ductile mechanism [3]. Aluminum–matrix composites generally have much lower ductilities than unreinforced Al. Heat treating to the T6 condition reduces ductility further [24–26]. Although it is clear that target ductility plays an important role in erosion [18,27,28], hardness is also important [2,3,29,30]. The data presented can be analyzed in terms of these competing factors, ductility decreases caused by hardness increases.

Fig. 6 – SEM micrographs of damage sites for 143 μm particles impacting at 15° and 100 m/s, (a) heat treated Al, (b) heat treated Al/SiC; the wear track is disrupted by a cluster of SiC's; μm markers are shown.

Effects of erodent size, D, on ΔW are shown in Fig. 4. For ductile metals, erosion rate generally increases with impacting particle size until some threshold particle size is reached. Further increases in particle size have no effect on erosion rate. Typical threshold values are about 100 μm, and the threshold appears to increase with increasing velocity [8,31]. The heat treated materials have lower strains to failure than do the as cast materials. It is possible that ductility influences the threshold D value. The strains induced

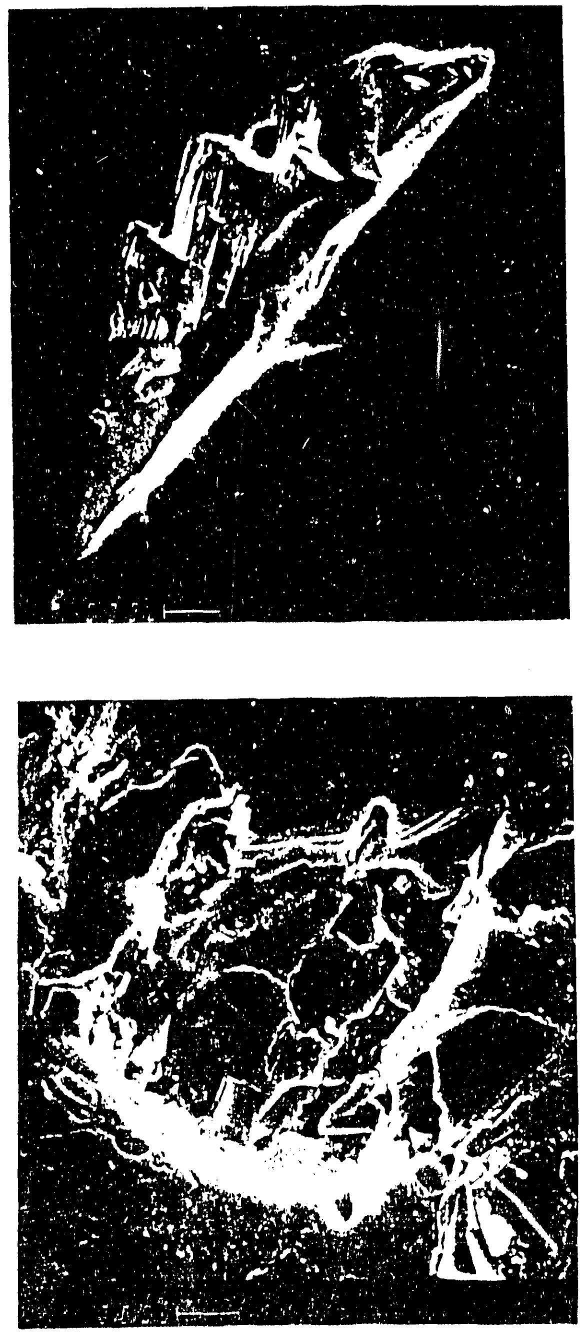

Fig. 7 – SEM micrographs of damage sites for 143 μm particles impacting at 90° and 100 m/s, (a) heat treated Al, (b) heat treated Al/SiC; μm markers are shown.

by small particles [illegible] small. For a given impact, [illegible] but little of it will reach the [illegible] and be removed. Material that [illegible] removed, by an impact will contribute to subsequent erosion resistance. Strains induced by particles above a certain size will be sufficient to cause material removal with the first impact. Thus, erosion rates will be expected to increase with particle size, until the particles become sufficiently large for material to be effectively removed by a single impact. Since failure strain will be affected by temperature, interplay between adiabatic heating [32] and strain to failure may be responsible for the observed dependencies of erosion rate on D.

Velocity exponents, n, were calculated from linear least-square fits to the log ΔW versus log V data. Some of the plots exhibited significant apparent curvature, which imparts a degree of uncertainty to the n values. The n values were generally independent of impact angle and all were within experimental error of those predicted in models of ductile erosion [3]. Heat treatment caused n to increase appreciably. Independence of n from impact angle has generally been observed for metals. Morrison et al. [8] point out that ductile erosive processes occur at all angles. Ploughing, cutting, indenting, and tearing may be more or less effective for different angles of impact, but each will occur. Thus erosion rate may change, as efficiencies of removal processes change, but functional relationships do not in general change because the basic mechanisms remain unchanged. This argument appears to apply to 2014 Al and, to some extent, to the Al-matrix composites.

The higher n values associated with heat treatment may be related to failure strains. For low kinetic energies, strains from impact are small and the lower ductilities of the hardened specimens relative to the as-received specimens do not lead to enhanced erosion. Both types of specimen have adequate ductility. For higher kinetic energies, the strains may be larger. If so, the reduced ductilities of the hardened materials would cause more severe wastage by ductile fracture. The ductilities of the as-received materials are sufficient to mitigate this ductile fracture. Higher n values in hardened materials result from enhanced erosion when impact energies are large.

Steady-state erosion surfaces of the Al were characterized by ductile ploughing. The composite surfaces were a mixture of ductile ploughing and tearing. Few reinforcement particles remained on the surface, which may imply that wholesale removal of ceramic particles that have separated from the matrix is a principal part of the material removal process. No significant difference was observed between the Al/SiC and Al/Al_2O_3. The overall appearances of the steady-state surfaces is of gouged and extruded metal, which is typical for erosion of ductile materials [8,33].

Observations of single impact sites and steady-state surfaces agree with the erosion data. For Al impacted at 15°, material is displaced by the initial impact. A pile-up is created at the end of a ploughed trail. For many of the impacts, the resultant pile is only loosely bonded to the remaining material, and it is clear that a second impact will remove the pile. Impact sites were similar for the as-cast and heat-treated Al. The only difference observed was that the grooves in the ploughed trails were continuous for the as-cast Al, but often slightly discontinuous for the heat-treated Al. The discontinuities appear to be slight tears, probably caused by the lower ductility of the heat-treated Al.

Impacts at 15° into the composites caused some fracture of, and tearing near, the ceramic reinforcement. For impact by smaller particles, little damage was generally observed. When the erodent struck in regions where the matrix was constrained by ceramic particles, appreciable material was removed. These areas correspond to regions where reinforcement particles were segregated because of dendrite formation during casting. The severely reduced local ductility due to the segregates appears to largely responsible for the higher erosive wear of the composites.

The results of the three materials for impacts at 90° were similar to those for 15°. Significant tearing was observed in the composites, but not in the Al. Shear bands, indicative of constrained plastic deformation, were only observed in the composites. Regions of metal surrounded by reinforcement particles were most easily removed by impact. It may be speculated that improvements in processing that produce uniform reinforcement distributions will improve erosion resistance significantly.

The data indicate that heat treatment influences erosion rate for 90° impact more than for 15° impact. Normal incidence induces more lateral displacement and less cutting than does glancing incidence [8]. For material removal by erosion, ductility considerations are likely to be of primary importance for lateral displacement events. For cutting events, resistance to penetration will also be important. Thus higher hardness will effectively compensate for lower ductility at glancing incidence, but strain to failure will dominate for normal incidence.

The erosion rates of the Al/SiC and Al/Al_2O_3 were virtually the same. Erosion rates of monolithic SiC and Al_2O_3 can vary by nearly an order of magnitude. It appears that erosion rate of Al–matrix composites will not be strongly influenced by the composition of the particulate ceramic reinforcement. Development of erosion–resistant alloys should focus on improving microstructural homogeneity and increasing ductility. Although high strength and ductility are clearly desirable properties, direct comparisons between erosion studies, and hence between materials, indicates that the product of strength and ductility is not always useful in predicting erosion rate [34–37]. The reinforcement phase should be well dispersed and should not have sharp edges. Especially for erosion at normal incidence, ductility is more important to erosion resistance than is strength and should be maximized for optimal erosion resistance.

CONCLUSIONS

Erosion data and SEM observations revealed that weight loss was more severe for Al/SiC and Al/Al_2O_3 composites than for the unreinforced 2014 Al alloy. Lack of ductility was the primary cause of the reduced erosion resistance of the composites. Regions of matrix constrained by the reinforced particles appeared to be most susceptible to wastage. Heat treatment increased hardness, but decreased ductility. Erosion rates were generally larger for the heat–treated materials.

ACKNOWLEDGMENTS

This work was supported by the U. S. Department of Energy, Office of Basic Energy Sciences, Division of Materials Science, under Contract W–31–109–Eng–38. The Al alloy and Al/SiC composites were provided by D. J. Lloyd of Alcan International and the Al/Al_2O_3 composites were provided by T. Klimowicz of Dural Aluminum.

REFERENCES

1. Natesan, K. "Corrosion–Erosion Behavior of Materials", The Metallurgical Society, Warrendale, Pennsylvania (1980)
2. Preece, C. M. and N. H. Macmillan, Ann. Rev. Mater. Sci. 7, 95–121 (1977)
3. Ruff, A. W. and S. M. Wiederhorn, Treat. Mater. Sci. Tech. 16, 69–126 (1979)
4. Roebuck, B., T. A. Gorley and L. N. McCartney, Mater. Sci. Tech. 5, 105–117 (1989)
5. Rohatgi, P., Adv. Mater. Proc. 136 [2], 39–44 (1990)
6. Evans, A. G., Mater. Sci. Eng. A107, 227–239 (1989)
7. Evans, A. G. and D. B. Marshall, Acta Metall. 37, 2567–2583 (1989)
8. Morrison, C. T., R. O. Scattergood and J. L. Routbort, Wear 111, 1–13 (1986)
9. Sundarajan, G. and P. G. Shewmon, Wear 84, 237–258 (1983)
10. Goretta, K. C., J. L. Routbort, A. Mayer and R. B. Schwarz, J. Mater. Res. 2, 818–826 (1987)
11. Lawn, B. R. and T. R. Wilshaw, J. Mater. Sci. 10, 1049–1081 (1975)
12. Evans, A. G., M. E. Gulden and M. E. Rosenblatt, Proc. Roy. Soc. London Ser. A361, 343–365 (1979)
13. Wiederhorn, S. M. and B. R. Lawn, J. Am. Ceram. Soc. 62, 66–70 (1979)
14. Sykes, M. T., R. O. Scattergood and J. L. Routbort, Composites 18, 153–163 (1987)
15. Morrison, C. T., J. L. Routbort and R. O. Scattergood, Mater Res. Soc. Symp. Proc. 78, 207–214 (1987)
16. Sheldon, G. L., Trans. ASME J. Basic Eng. 92, 619–626 (1970)
17. Srinivasan, S. and R. O. Scattergood, J. Mater. Sci. 22, 3463–3469 (1987)
18. Wu, W., K. C. Goretta, P. K. Rohatgi, S. Mostovoy and J. L. Routbort, In "Proc. Industry–University Advanced Materials Conference II," F. W. Smith, ed., pp. 100–107, Advanced Materials Institute, Golden, Colorado, (1989)
19. Lloyd, D. J., H. Lagace, A. McLeod and P. L. Morris, Mater. Sci. Eng., A107, 73–80 (1987)
20. Krautkrämer, J. and H. Krautkrämer, "Ultrasonic Testing of Materials," Springer–Verlag, New York, New York (1983)

21. Kosel, T. H., R. O. Scattergood and A. P. L. Turner, In "Wear of Materials 1979," K. C. Ludema, W. A. Glaeser, and S. K. Rhee eds., pp. 192–204, American Society of Mechanical Engineers, New York, New York (1979)
22. Routbort, J. L., C.–Y. Chu, J. P. Singh and K. C. Goretta, J. Hard Mater, 1, in press (1990)
23. Routbort, J. L. and Hj. Matzke, J. Mater. Sci. 18, 1491–1496 (1983)
24. Nair, S. V., J. K. Tien and R. C. Bates, Inter. Met. Rev. 30, 275–290 (1985)
25. Lewandowski, J. J., C. Liu and W. H. Hunt, Jr., Mater. Sci. Eng. A107, 241–255 (1989)
26. Kamat, S. V., J. P. Hirth and R. Mehrabian, Acta Metall. 37, 2395–2402 (1989)
27. Levy, A. V., In "Proceedings of 5th International Conference on Erosion by Liquid and Solid Impact," J. E. Field ed., Paper 39, Cambridge University Press, Cambridge, United Kingdom (1979)
28. Ninham, A. J. and A. V. Levy, Wear 121, 347–361 (1988)
29. Finnie, I., J. Wolak and Y. Kabel, J. Mater. 2, 682–700 (1967)
30. Sheldon, G. L., J. Eng. Mater. Tech. 99, 133–137 (1977)
31. Goodwin, J. E., W. Sage and G. P. Tilly, Proc. Inst. Mech. Engrs. 184, 279–289 (1969)
32. Shewmon, P. G., Wear 68, 253–258 (1981)
33. Levy, A. V., Wear 108, 1–21 (1986)
34. Hovis, S. K., J. Talia and R. O. Scattergood, Wear, 1986, 107, 175–181 (1986)
35. Hovis, S. K., J. E. Talia and R. O. Scattergood, Wear 108, 139–155 (1986)
36. Aptekar, S. S. and T. H. Kosel, In "Wear of Materials 1985," K. C. Ludema, ed., pp. 677–686, American Society of Mechanical Engineers, New York, New York (1985)
37. Srinivasan, S., R. O. Scattergood and R. Warren, Metall. Trans. 19A, 1785–1793 (1988)

END

DATE FILMED

01 / 29 / 91